Microelectronic Engineering 133 (2015) 45–50

Contents lists available at ScienceDirect

Microelectronic Engineering

journal homepage: www.elsevier.com/locate/mee

Characterization of stable and transient cavitation in megasonically irradiated aqueous solutions ☆

Rajesh Balachandran [a], Mingrui Zhao [b], Petrie Yam [c], Claudio Zanelli [c], Manish Keswani [a,*]

[a] Materials Science and Engineering, University of Arizona, Tucson, AZ, USA
[b] Chemical and Environmental Engineering, University of Arizona, Tucson, AZ, USA
[c] Onda Corporation, Sunnyvale, CA, USA

ARTICLE INFO

Article history:
Received 2 June 2014
Received in revised form 24 November 2014
Accepted 25 November 2014
Available online 29 November 2014

Keywords:
Megasonic cleaning
Stable cavitation
Transient cavitation
Hydrophone
Hydroxyl radical

ABSTRACT

Megasonic cleaning is routinely used for removal of particulate contaminants from various surfaces in integrated circuit industry. One of the drawbacks of megasonic cleaning is that although it can achieve good particle removal efficiencies at high power densities, it also causes feature damage. The current paradigm is that damage is primarily caused by transient cavitation whereas cleaning is affected by streaming and stable cavitation. In order to develop a damage-free and effective megasonic cleaning process, it is essential to understand the acoustic bubble behavior and identify conditions that generate significant stable cavitation without any transient cavitation. In the current work, microelectrode based chronoamperometry, pressure measurements using a hydrophone and fluorescence spectroscopy studies were conducted under different acoustic frequencies (1–3 MHz) and power densities (2–8 W/cm^2) to fundamentally investigate the type of cavitation produced under these conditions and also establish a correlation to the generation of hydroxyl radicals for characterization of transient cavitation.

1. Introduction

Megasonic cleaning has been widely used in the integrated circuit (IC) industry as an intermediary step for surface preparation of processes such as thin film deposition, etching, chemical mechanical planarization (CMP), lithography and others [1]. As the technology node in the semiconductor industry moves towards smaller sizes, the demand for efficient megasonic cleaning processes that can effectively remove particles with minimum damage arises. Considerable work has been done on fundamentally characterizing the cavitation behavior at frequencies in the range of about 0.8–1 MHz [2–5]. Kumari et al. [2] conducted damage studies on two types of patterned substrates (array of lines of high k-metal gate stacks on silicon and poly-Si lines on silicon) at a frequency of about 0.925 MHz by varying the power density (0.15–2.94 W/cm^2) and amount of dissolved CO_2 (0.5–1035 ppm). For both structures, it was observed that there was significant damage observed in air saturated solutions while CO_2 saturated solutions (1035 ppm CO_2 in DI water) showed minimal damage. The authors hypothesized that CO_2 due to its higher solubility than air diffuses into the cavity in higher amounts and cushions the collapse, which significantly suppresses transient cavitation. In another study on investigating the role of various dissolved gases (Ar, N_2, CO_2) on transient cavitation at ~1 MHz sound field using high time resolution cyclic voltammetry studies, it was illustrated that the frequency of occurrence and intensity of transient cavitation was lowest in CO_2 containing aqueous solutions and highest in Ar saturated solutions [3]. Kang et al. [4] conducted particle removal and damage studies on patterned photoresist and polysilicon structures at operating frequency of ~0.8 MHz in DI water solutions containing different concentrations of dissolved gases (Ar, O_2, N_2 and H_2). The operating power was maintained constant at 70% of the maximum value. They showed that as the partial pressure of the dissolved gases increased, the particle removal efficiency and the number of damaged structures also increased. These studies emphasize the importance of dissolved gases on cavitation activity. It is generally believed [6] that the intensity of transient cavitation is much lower at higher acoustic frequencies and may offer a viable solution to damage-free and effective cleaning. Although there are several reported studies on particle removal, feature damage and the driving mechanisms at an acoustic frequency of ~1 MHz, there is little information available on cavitation behavior at higher frequencies (2–4 MHz).

In a study on the effect of megasonic frequency at ~3 MHz on cleaning efficiency, Kim et al. [1] developed a near-field megasonic waveguide consisting of a small cylindrical lead zirconate titanate

☆ This paper was submitted for 2014 SPCC.

* Corresponding author. Tel.: +1 (520) 270 4361.
E-mail address: manishk@email.arizona.edu (M. Keswani).

http://dx.doi.org/10.1016/j.mee.2014.11.020
0167-9317/

(PZT) actuator for effective removal of nanoparticles from silicon wafers. The results revealed that the average maximum pressure values obtained from the new waveguide were about 35.6% lower with more uniform pressure field distribution compared to that from a traditional waveguide, indicating a possible decrease in the degree of transient cavitation and therefore pattern damage. Shende et al. [7–9] studied the effect of different dissolved gases (Ar, CO_2 and H_2) on the acoustic pressure, sonoluminescence and pattern damage on phase shift masks with aspect ratios in the range of 1:1 to 1.8:1 under different acoustic frequencies (1–4 MHz) and transducer powers. The effect of varying the frequency in the range of 1–4 MHz [8,9] was quite evident for DI water cleaning solution where the damage was lowest at 4 MHz suggesting a significant reduction of transient cavitation at this frequency.

Yasui [10] simulated the bubble behavior under different frequencies to understand the effect of controlling parameters behind cavitation. His work revealed that the range of the ambient bubble radius for sonoluminescing cavitation bubbles narrows as the ultrasonic frequency increases from 20 kHz to 1 MHz. Another study [11] indicated that the pressure amplitude of the megasonic wave must be in the range of about 100–400 kPa for stable cavitation to be dominant. It was reported in this work that effective particle removal with minimal damage could be achieved by maximizing the extent of stable cavitation and eliminating any occurrence of transient cavitation.

In this study emphasis has been laid on fundamentally understanding the cavitation behavior under applied acoustic frequencies of 1 and 3 MHz and transducer power densities of 2–8 W/cm^2, as estimated by the electrical power input from the generator and the area of the transducers. Primarily, cavitation investigations have been carried out by means of a microelectrode based electrochemical sensor in solutions containing ferricyanide as the electroactive species. Supporting pressure measurements were conducted using a hydrophone to confirm the extent of transient cavitation under different experimental conditions. Finally, fluorescence spectroscopy was performed to determine the rate of generation of OH radicals, which is further an indicator of the degree of transient cavitation.

2. Materials and methods

High resistivity de-ionized water (18 MΩ-cm) was used for all experiments. Potassium ferricyanide, potassium chloride, terephthalic acid and 2-hydroxy terephthalic acid were greater than 99% purity and purchased from Sigma Aldrich Inc. VLSI grade ammonium hydroxide (29%) was procured from Honeywell Inc. Megasonic experiments were performed in Mini-meg® tanks (PCT Systems Inc.) of volume ~4.5 l consisting of 125 cm^2 transducers affixed at the bottom with operating frequencies of 1 and 3 MHz. Chronoamperometry experiments were conducted with a microelectrode (12.5 μm radius) in 50 mM potassium ferricyanide ($K_3Fe(CN)_6$) solutions with 100 mM potassium chloride (KCl) as the supporting electrolyte. The solutions were saturated with argon gas for 30 min and a blanket was maintained to prevent diffusion of O_2 into the solution. The microelectrode set-up consists of three electrodes namely, working (25 μm diameter Pt disc), reference and counter (500 μm diameter Pt wires) placed in a triangular fashion with a spacing of 0.4 cm between them [12]. High sampling rates (4 million samples/s) were achieved by using an oscilloscope (NI USB 5133) in tandem with a potentiostat (Gamry Interface 1000). Labview® and Diadem® software (National Instruments) were used to acquire and analyze the high sampling rate data. Pressure measurements in the megasonic tank were achieved by means of a hydrophone (HCT-0310, Onda Corp.). The hydrophone consists of pressure sensitive tip (diameter ~1 mm) which is acoustically isolated from the rest of the probe to localize the measurement. Data was collected as a function of time at sampling rate of 50 million samples/s using a similar setup as that for the chronoamperometry experiments. Discrete Fourier Transform (DFT) applied to the voltage–time data transformed it to frequency domain, which was further adjusted using the hydrophone calibration. Subsequently, hydroxyl radical (OH·) measurement experiments were conducted in dilute (1:10,000 by volume) NH_4OH (29%):DI water solution (pH = 8.7) containing 75 μM terephthalic acid (TA) using fluorescence spectroscopy (FluroMax 4, Horiba Inc.) [13]. The alkaline pH of the solution was necessary to achieve complete dissolution of TA. In the presence of applied megasonic field, the terephthalic acid reacts with the generated OH· to form 2-hydroxyterephthalic acid which under a suitable excitation field (318 nm) undergoes emission (425 nm). The fluorescence intensity was related to amount of OH· released using a calibration curve (shown in Fig. 1) generated by measuring fluorescence from aqueous solutions containing known concentrations of 2-hydroxyterephthalic acid.

3. Results and discussion

3.1. Cavitation behavior at 1 MHz

Fig. 2(a) and (b) show current as a function of time at an operating frequency of 1 MHz and two different power densities of 2 and 8 W/cm^2, respectively. The current data in the presence and absence of megasonic field in each plot are marked appropriately. It may be noted that in the absence of applied megasonic field, a baseline current of about −0.4 μA was observed. This baseline current pertains to the reduction of ferricyanide to ferrocyanide as per the following reaction (R1):

$$[Fe(CN)_6]^{3-} + e^- \rightarrow [Fe(CN)_6]^{4-} \quad (R1)$$

In the presence of megasonic field, current peaks (or actually inverse current peaks) were observed. These peaks have been attributed to transient cavitation events [3]. It could be seen that as the power density was increased from 2 W/cm^2 to 8 W/cm^2, the number of current peaks and their magnitude increased. This observation is in agreement with the fact that the number of transient cavities increase with increasing power density. Further, to better understand the behavior of the bubble, the expanded time scale of typical current peaks is shown in Fig. 2(c) and (d). The rise and fall in current correspond to the diffusion of electroactive species from the imploding cavity towards the microelectrode. The rise and fall times for a transient cavity at 2 W/cm^2 were measured

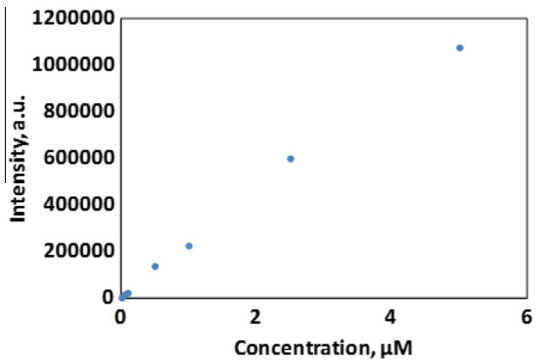

Fig. 1. Calibration curve for fluorescence intensity as a function of 2-hydroxyterephthalic acid concentration, excitation wavelength = 318 nm, emission wavelength = 425 nm, slit size = 2 nm.

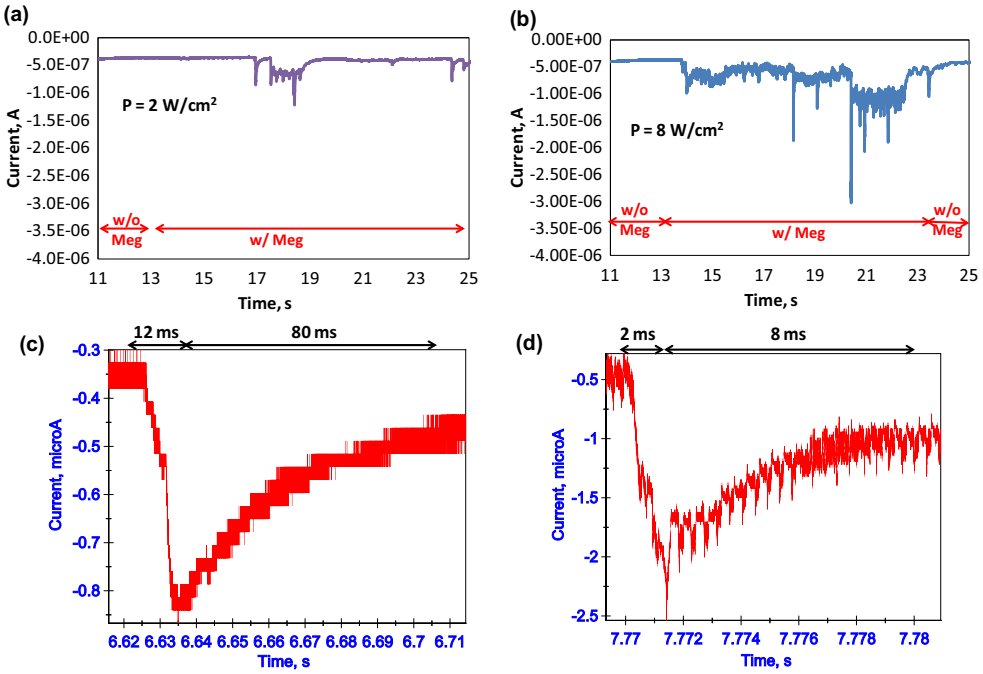

Fig. 2. Chronoamperometry data obtained at an acoustic frequency of 1 MHz and power density of (a) 2 W/cm^2, (b) 8 W/cm^2, (c) expanded time scale at 2 W/cm^2 and (d) expanded time scale at 8 W/cm^2.

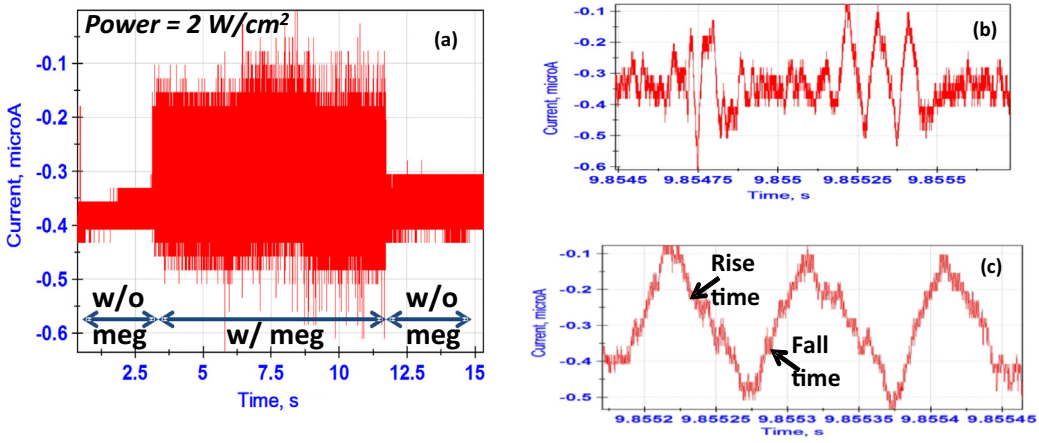

Fig. 3. (a) Chronoamperometry data at acoustic frequency of 3 MHz and power density of 2 W/cm^2 and (b) and (c) current data with expanded time scale.

to be in the range 10–20 ms and 60–80 ms, respectively, which are in reasonable agreement with that reported in [3]. Interestingly, at higher power density of 8 W/cm^2, the rise and fall times were in the range of 2–5 ms and 8–15 ms, respectively. This reduction in time could possibly be attributed to higher acoustic streaming present at higher powers, which causes faster dispersion of ferricyanide towards the electrode surface.

3.2. Cavitation behavior at 3 MHz

Fig. 3(a) through (c) show the chronoamperometry data obtained at an acoustic frequency of 3 MHz and power density of about 2 W/cm^2. The first 3 s of the data represents the baseline current in the absence of applied megasonic field. It could be seen that the baseline current in this case was also about −0.4 μA. In the presence of the megasonic field, a discrete behavior was observed. The current peaks were observed on both sides (negative and positive) of the baseline current. This behavior is a characteristic of that seen at 3 MHz, while cavitation data at 1 MHz showed current peaks of increasing magnitude (more negative current) that was typical of transient cavities. In order to further understand the cavitation behavior at 3 MHz, expanded time scales of the chronoamperometry data has been plotted in Fig. 3(b). Current peaks exhibiting an oscillatory behavior were observed. This oscillatory behavior may be attributed to the existence of stable cavities. The shift of current in the positive side of the baseline current (from −0.4 μA to −0.1 μA) could possibly be due to the blocking of the electrode as the oscillating bubble expands. On contraction, the bubble shrinks thereby unblocking the electrode and also causing the transport of ferricyanide ions towards the electrode by microstreaming thereby increasing the current value from about −0.1 μA to −0.5 μA. It is important to point out that for such a blocking/unblocking behavior to be observed, the bubble must be present in the close vicinity of the electrode surface which did not seem to be the case at 1 MHz. Also, as seen from Fig. 3(c), the rise and fall times of the oscillating current were about

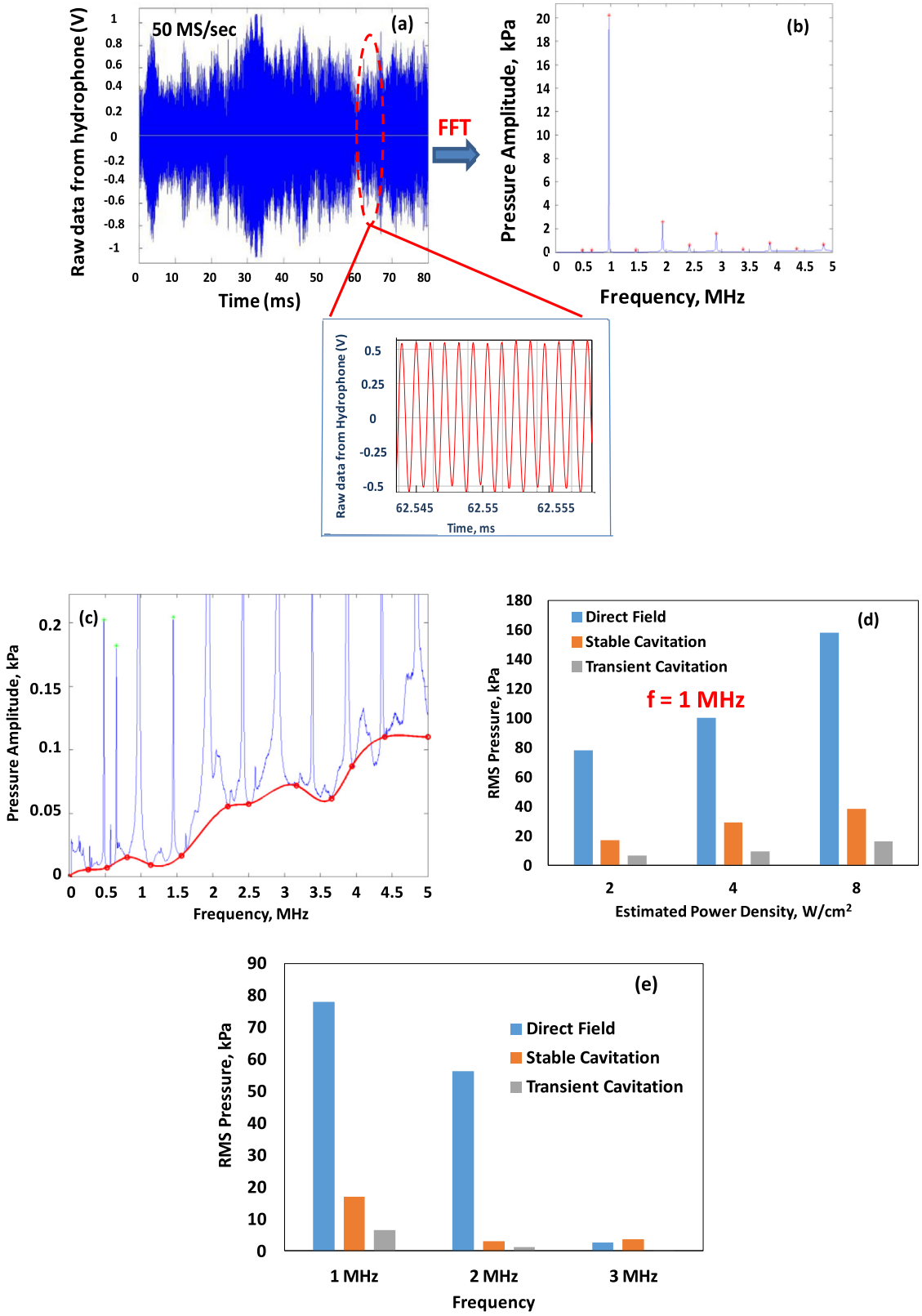

Fig. 4. (a) Raw data obtained from the hydrophone at sampling rate of 50 MS/s (inset: expanded time scale of the raw data), (b) converted data in the frequency domain after Fourier transform and correction for the hydrophone sensitivity, (c) expanded *y*-axis showing the broadband spectrum, (d) RMS pressures of direct, stable cavitation and transient cavitation fields as a function of power density at an acoustic frequency of 1 MHz and (e) RMS pressures direct, stable cavitation and transient cavitation fields as a function of acoustic frequency (1–3 MHz) at a transducer power density of 2 W/cm^2.

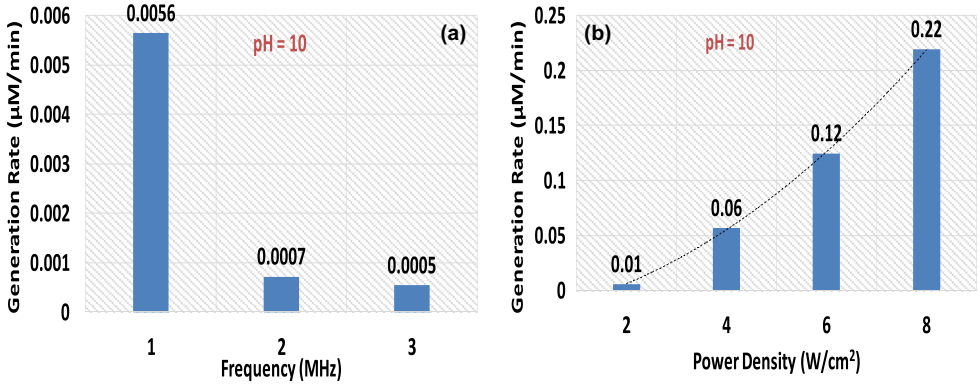

Fig. 5. Hydroxyl radical generation rate as a function of (a) megasonic frequency at power density of 2 W/cm^2 and (b) power density at an operating frequency of 1 MHz.

30–50 μs, almost three orders of magnitude lower than that seen at 1 MHz. It is known that with increase in acoustic frequency, the transient cavitation threshold also increases [14]. Therefore, at higher frequencies, most of the bubbles do not transform into transient cavities but are present as stable cavities. The results obtained from chronoamperometry studies also corroborate the presence of predominantly stable cavities at higher frequencies.

3.3. Pressure measurements using a hydrophone

Fig. 4(a) shows the raw data obtained from the hydrophone in the form of voltage as a function of time in air saturated aqueous solutions subjected to megasonic field. As can be noticed from the inset of this figure, which displays the voltage values with expanded time scale, the primary oscillations occur at the driving frequency (in this case ~1 MHz). By using the hydrophone calibration chart consisting of voltage per unit pressure versus frequency as provided by the manufacturer, the measured voltage was converted into pressure followed by application of the discrete Fourier transform (DFT) to obtain the data in the frequency domain. Fig. 4(b) shows the transformed data in the frequency domain, with a prominent sharp peak at about 1 MHz, the driving frequency of the transducer.

The integral under this fundamental peak (above the background) was computed as the pressure generated (root mean square, RMS) by the direct field as it arises from the fundamental pressure wave of the transducer as well as scattered pressure from the resonating bubbles. Subsequent harmonics with decreasing pressure amplitude were observed at ~2, 3 MHz and higher order. These peaks and those observed at the sub-harmonic (half-order harmonic at 0.5 MHz) and ultra-harmonics (~1.5, 2.5, 3.5, ... MHz) represent non-linearly oscillating stable bubbles or the inherent non-linearity of the medium. The half-order harmonic often may occur in short bursts separated by long intervals and therefore at low average levels. The collective integral under these peaks (above the background) was attributed to the pressure generated due to the stable cavitation. Characterization of transient cavitation was conducted by investigating the lower amplitude region of the Fig. 4(b) by expanding the *y*-axis scale. Fig. 4(c) shows that the line spectrum, indicative of the stable cavitation, is superimposed on a continuous broadband spectrum, a form of acoustic noise. This part of the spectrum emerges from random transient cavitation events that generate high pressure shock waves from a collapsing bubble (transient cavity) in the vicinity of the hydrophone. The broadband spectrum was fit using a Matlab routine (shown by the red curve). The integral under the red curve gives a measure of root mean square pressure due to transient cavitation [15,16]. Fig. 4(d) shows the RMS pressures from direct field, stable cavitation and transient cavitation as a function of varying power densities in air saturated DI water at an acoustic frequency of 1 MHz. It could be seen that the direct field pressure has a higher magnitude in comparison to that from stable and transient cavitation and the behavior was independent of power density and frequency (Fig. 4(e)). This indicates that most of the pressure arises from resonating bubbles (which are typically 3 μm in radius at ~1 MHz [17]) and from the primary acoustic wave of the transducer for megasonic frequencies. As the power density was increased from 2 to 8 W/cm^2, only a twofold increase in direct field pressure from 80 to 160 kPa was observed, while a similar increase in pressures of stable and transient cavitation was also measured. This indicates that the increase of non-linear stable cavitation and transient cavitation events is more rapid at higher power densities due to transformation of direct pressure field energy to higher energy cavitation events. This effect was also evident from microelectrode studies where the increase in number of transient cavities was higher at higher power densities. Fig. 4(e) shows the effect of acoustic frequency on the RMS pressure generated at a fixed power density of 2 W/cm^2. Direct field pressure shows a decrease by about an order of magnitude (from about 80 to 5 kPa) as the acoustic frequency was increased from 1 to 3 MHz. A similar decrease of stable cavitation and transient cavitation pressures was observed with increase of frequency from 1 to 2 MHz with complete elimination of transient cavitation pressure at 3 MHz suggesting absence of high energy cavitation events at this frequency. This result corroborates with those observed from microelectrode studies wherein stable cavitation was dominant at 3 MHz.

3.4. Hydroxyl radical capture measurements

The degree of transient cavitation could also be predicted by measuring the amount of hydroxyl radicals generated during megasonic exposure. Fluorescence spectroscopy was used to measure the concentration of 2-hydroxyterephthalic acid formed as a result of the reaction (R2) of terephthalic acid with OH· generated predominantly inside or surrounding a collapsing cavity when the temperature reaches a few thousand degrees.

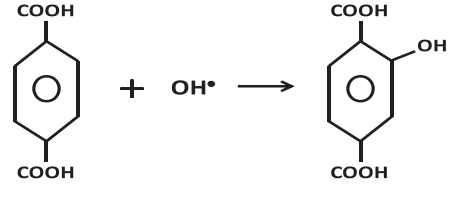

(R2)

Fig. 5 shows the generation rate of OH· as a function of acoustic frequency and power density. The accuracy of OH· measurement was ~0.1 nM/min. The effect of frequency at fixed power density

of 2 W/cm^2 (Fig. 5(a)), indicates that as the frequency is increased the generation rate of OH$^\cdot$ falls down significantly from about 5 nM/min at 1 MHz to about 0.5 nM/min at 3 MHz. The small but measurable value of rate of generation of OH$^\cdot$ at 2 and 3 MHz is likely due to a few non-linearly oscillating stable cavities with high amplitudes that exist at these frequencies and offer temperature conditions just sufficient for generation of OH$^\cdot$ from decomposition of water. These results clearly suggest that the degree of transient cavitation is much lower at higher frequencies and complements the results obtained from pressure measurements and chronoamperometry studies. Fig. 5(b) shows that as the power density at 1 MHz increased from 2 to 8 W/cm^2, the OH$^\cdot$ generation rate increased from about 10 nM/min to 220 nM/min, which corroborates with the increase of transient cavitation intensity at higher power densities as measured using the hydrophone.

4. Conclusions

High time resolution chronoamperometry experiments, hydrophone pressure measurements and OH$^\cdot$ capture experiments were performed to characterize the cavitation behavior in the frequency range of 1–3 MHz and power densities of 2–8 W/cm^2. Microelectrode investigations showed that at higher frequencies of ~3 MHz, stable cavitation was dominant while transient cavitation was characteristic at 1 MHz. As the acoustic frequency was increased from 1 to 3 MHz, pressure measurements revealed a decrease in relative transient cavitation intensity by two orders of magnitude, while the hydroxyl capture study showed a decrease in OH$^\cdot$ generation rate by an order of one. This study concludes that transient cavitation decreases with increasing acoustic frequency (1–3 MHz) and decreasing power density. Since damage is caused by transient cavitation while cleaning can be achieved by both stable and transient cavitation, an optimum megasonic frequency and power density will likely offer necessary conditions for effective cleaning without any feature damage. It may be noted that the results in this study are based on a specific megasonic system and therefore further validation of this work through cleaning/damage studies will be beneficial.

Acknowledgements

The authors would like to acknowledge University of Arizona (Grant # 1127508) and Water, Environmental and Energy Solutions (Grant # 5825632) for providing financial support for this research work. We would also like to express gratitude to PCT Systems (Scott Osterman and Sharyl Maraviov) for their support with the megasonic systems.

References

[1] H. Kim, Y. Lee, E. Lim, Design, fabrication and performance test of a 3 MHz megasonic waveguide for nano-particle cleaning, in: Proc. of the 13th IEEE International Conference on Nanotechnology, 2013, pp. 633–636.
[2] S. Kumari, M. Keswani, S. Singh, M. Beck, E. Liebscher, L.Q. Toan, S. Raghavan, ECS Trans. 41 (5) (2011) 93–99.
[3] M. Keswani, S. Raghavan, P. Deymier, Microelectron. Eng. 102 (2013) 91–97.
[4] B.-K. Kang, M.-S. Kim, S.-H. Lee, H.-S. Sohn, J.-G. Park, ECS Trans. 41 (5) (2011) 101–107.
[5] M. Hauptmann, H. Struyf, P. Mertens, M. Heyns, S. De Gendt, C. Glorieux, S. Brems, AIP Conf. Proc. 1433 (2012) 299–303.
[6] M. Ashokkumar, J. Lee, Y. Iida, K. Yasui, T. Kozuka, T. Tuziuti, A. Towata, Phys. Chem. Chem. Phys. 11 (2009) 10118–10121.
[7] H. Shende, S. Singh, J. Baugh, W. Dietze, P. Dress, Proc. SPIE 8701 (870105) (2013) 1–7.
[8] H. Shende, S. Singh, J. Baugh, R. Mann, U. Dietze, P. Dress, Proc. SPIE 8166 (816614) (2011) 1–10.
[9] H. Shende, S. Singh, J. Baugh, U. Dietze, P. Dress, Proc. SPIE 8522 (852217) (2012) 1–7.
[10] K. Yasui, J. Acoust. Soc. Am. 112 (4) (2002) 1405–1413.
[11] K. Suzuki, Y. Imazeki, K. Han, S. Okano, J. Soejima, Y. Koike, Jpn. J. Appl. Phys. 50 (2011). 05EC10-1–05EC10-5.
[12] M. Keswani, S. Raghavan, P. Deymier, Ultrason. Sonochem. 20 (2013) 603–609.
[13] A. Sazgarnia, A. Shanei, Int. J. Photoenergy 2012 (2012) 1–5.
[14] O. Louisnard, J. Gonzalez-Garcia, Acoustic cavitation, in: H. Feng, G. Barbosa-Canovas, J. Weiss (Eds.), Ultrasound Technologies for Food and Bioprocessing, Springer Publishing, New York, 2010 (Chapter 2).
[15] L. Liu, Y. Yang, P. Liu, W. Tan, Ultrason. Sonochem. 21 (2014) 566–571.
[16] J. Frohly, S. Labouret, C. Bruneel, I. Looten-Bacquet, R. Torguet, J. Acoust. Soc. Am. 108 (5) (2000) 2012–2020.
[17] T. Leong, M. Ashokkumar, S. Kentish, Acoust. Aust. 39 (2) (2011) 54–63.